Speckle-metric-optimization-based adaptive optics for laser beam projection and coherent beam combining

Mikhail Vorontsov,[1,2,*] Thomas Weyrauch,[1] Svetlana Lachinova,[2] Micah Gatz,[1] and Gary Carhart[3]

[1]*Intelligent Optics Laboratory, School of Engineering, University of Dayton, 300 College Park, Dayton, Ohio 45469-2951, USA*

[2]*Optonicus, 711 E. Monument Avenue, Suite 101, Dayton, Ohio 45402, USA*

[3]*Intelligent Optics Laboratory, Computational and Information Sciences Directorate, United States Army Research Laboratory, 2800 Powder Mill Road, Adelphi, Maryland 20783, USA*

**Corresponding author: mikhail.vorontsov@udayton.edu*

Received April 9, 2012; accepted May 2, 2012;
posted May 8, 2012 (Doc. ID 166413); published July 4, 2012

Maximization of a projected laser beam's power density at a remotely located extended object (speckle target) can be achieved by using an adaptive optics (AO) technique based on sensing and optimization of the target-return speckle field's statistical characteristics, referred to here as speckle metrics (SM). SM AO was demonstrated in a target-in-the-loop coherent beam combining experiment using a bistatic laser beam projection system composed of a coherent fiber-array transmitter and a power-in-the-bucket receiver. SM sensing utilized a 50 MHz rate dithering of the projected beam that provided a stair-mode approximation of the outgoing combined beam's wavefront tip and tilt with subaperture piston phases. Fiber-integrated phase shifters were used for both the dithering and SM optimization with stochastic parallel gradient descent control.

OCIS codes: 010.1080, 010.1285, 140.3298.

Laser beam focusing into the smallest possible spot (target hit spot) at a remotely located object in atmosphere is the major objective for laser beam projection (directed energy) technology under development [1]. Achievement of this goal requires the efficient mitigation of atmospheric turbulence-induced phase aberrations with adaptive optics (AO) techniques [2]. In existing AO systems, the precompensation of the outgoing beam's phase aberration is performed using either optimization of a measured signal that is proportional to the target-return light power within the receiver aperture [power-in-the-bucket (PIB) metric, J_{PIB}], or sensing and conjugation of the target-return field's wavefront phase—phase-conjugate (PC) type AO control [3,4]. It is important to note that both AO control techniques are based on the assumption that the target is either unresolved, that is, is smaller than the diffraction-limited beam size, b_{dif}, or has a bright, unresolved, stationary glint. Here we consider a more realistic case of laser beam projection onto an extended (resolved) target with a randomly rough surface. The coherent beam scattering off the target's rough surface results in a strong speckle modulation at the transceiver plane. This speckle modulation represents a long-standing major challenge (known from the late 1970s as the speckle problem in AO) for utilization of both AO PIB metric optimization and PC control techniques [5–7]. In this Letter, we address this problem by introducing the speckle-metric (SM) optimization-based AO technique (SM AO) and describe experimental results that, to our knowledge, are the first successful demonstration of target-in-the-loop laser beam projection onto an extended target with a randomly rough surface.

In the SM AO technique proposed here, control of the outgoing laser beam phase is performed using optimization of speckle-averaged characteristics of the target-return speckle field, which are referred to here as SMs [8,9]. The term "speckle averaging" implies averaging the return-wave characteristic $J(t)$ over time τ_J, which exceeds significantly the characteristic time τ_{sp} of the speckle-field realization update inside the receiver aperture. In the SM AO technique, the speckle-field realization update occurs due to artificially induced hit-spot displacement (dithering) that is achieved by modulating (steering) the outgoing beam wavefront tip and tilt. The measured characteristic $J_{\mathrm{sp}} = \langle J \rangle_{\mathrm{sp}}$, where $\langle \ldots \rangle_{\mathrm{sp}}$ denotes speckle averaging, can be utilized for AO wavefront control as a performance measure (SM) if the following conditions are fulfilled: (a) J_{sp} depends monotonically on a target-plane beam quality metric J_T, which characterizes the power density distribution inside the target hit spot, and (b) J_{sp} can be obtained (measured) over a time τ_J that is considerably shorter than the characteristic times τ_{at} and τ_{AO} of turbulence and closed-loop AO control, respectively. Assume first that for a measured signal $J(t)$ and the corresponding speckle-average characteristic J_{sp} condition (a) is satisfied and consider the hierarchy of characteristic time scales following from (b), which is required for SM AO control implementation:

$$\tau_{\mathrm{sp}} \ll \tau_J \ll \tau_{\mathrm{AO}} \le \tau_{\mathrm{at}}. \tag{1}$$

To estimate the characteristic time τ_{sp} of the outgoing tip/tilt phase modulation that is used in the SM AO technique for speckle-field realization updates, assume in Eq. (1) that $\tau_{\mathrm{sp}} \approx 10^{-2}\tau_J \approx 10^{-4}\tau_{\mathrm{at}}$. With the commonly used estimate for the characteristic atmospheric time, $\tau_{\mathrm{at}} = 1$ ms, we obtain $\tau_{\mathrm{sp}} = 0.1$ μs. Note that fulfilling this condition requires tip/tilt phase modulation with hit-spot dithering frequencies, $\omega_{\mathrm{dith}} \sim 1/\tau_{\mathrm{sp}}$, in the 10 MHz range, which cannot be achieved using conventional optomechanical beam-steering mirrors.

In the SM AO approach, the required hit-spot dithering frequency is realized by using laser transmitters based on phased fiber arrays as shown in Fig. 1(a). The laser beam transmitter (beam director) is composed of densely packed fiber collimators that are optically coupled with a narrow-linewidth, multichannel master oscillator power amplifier (MOPA) system that utilizes single-mode

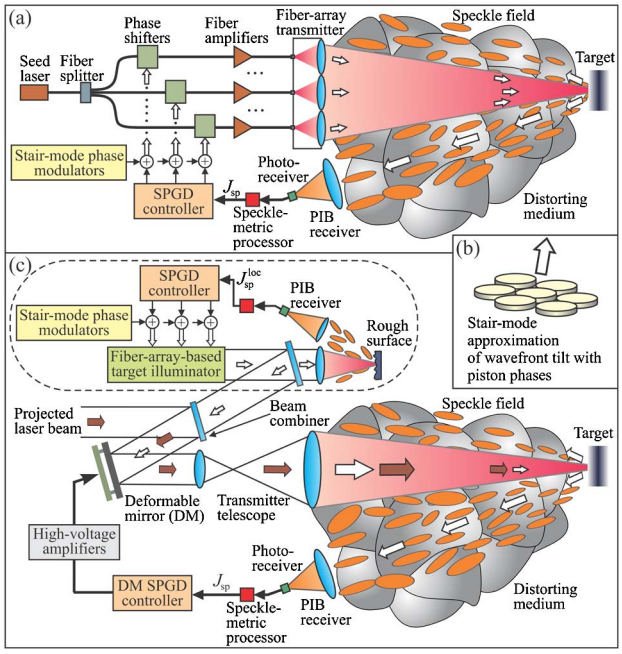

Fig. 1. (Color online) Laser beam projection systems with SM AO: (a) fiber-array-based and (c) conventional with fiber-array-based target illuminator (shown inside dashed frame). (b) Depiction of stair-mode tilt approximation.

polarization-maintaining fibers [10]. Each channel of the MOPA system includes a $LiNbO_3$ fiber-integrated phase shifter capable of GHz-rate control of the piston phase of the beam transmitted through its corresponding fiber collimator. The high-frequency hit-spot dithering required for SM AO can be achieved in this system using a piston-wise (stair-mode) approximation of the outgoing beam wavefront tilts as illustrated in Fig. 1(b). Note that dithering of the outgoing beam also results in an undesired overall increase of the projected beam's long-exposure hit-spot footprint and the corresponding decrease of the time-averaged power density. For this reason, the stair-mode dithering amplitude should be small but still large enough to provide a statistically representative ensemble of uncorrelated (or at least weakly correlated) speckle-field realizations that can be used for SM evaluation. A small dithering amplitude is also important for mitigation of anisoplanatic effects [11]. As analysis and experiments show, the hit-spot dithering with amplitudes $b_{\text{dith}} \approx 0.75 b_{\text{dif}}$ to b_{dif} represents an acceptable compromise between the factors mentioned above [11].

Due to the high bandwidth of the fiber-integrated phase shifters they can be used for both hit-spot dithering and SM optimization leading to coherent combining (phasing) of the outgoing beams at the target plane. This fiber-array beam projection system with SM AO control is shown in Fig. 1(a). SM optimization in this system is performed using the stochastic parallel gradient descent (SPGD) control algorithm [12]. In a beam projection system with a conventional laser transmitter telescope as shown in Fig. 1(c), the phased fiber array is utilized as a target illuminator that uses hit-spot dithering solely for SM sensing. SM optimization in this SM AO system is achieved by shaping the outgoing beam's wavefront phase with a deformable mirror that is located in the common optical train for both the target illuminator and the projected laser beams. For efficient combining of these beams before entering the transmitter telescope, they should have slightly different wavelengths or orthogonal polarization states. For compensation of the MOPA-system-induced random phase shifts in the fiber-array illuminator in Fig. 1(c), the outgoing beams should be phased at the pupil plane, which can be achieved with an additional SM AO control system shown inside the dashed box in Fig. 1(c). This control system optimizes the local speckle metric, $J_{\text{sp}}^{\text{loc}}$, which is obtained by focusing a small portion of the illuminator beam onto a rough surface.

In the following, we show that signal processing of the PIB signal, $J_{\text{PIB}}(t)$, measured with a receiver telescope (PIB receiver) allows obtaining SMs, J_{sp}, that can be utilized for SM AO in the beam projection systems depicted in Fig. 1. The SMs considered here are derived from an analysis of the temporal correlation function of the time-varying component $\delta J_{\text{PIB}}(t)$ of the measured PIB signal $J_{\text{PIB}}(t)$: $\Gamma_{\text{PIB}}(\tau) \equiv \langle \delta J_{\text{PIB}}(t) \delta J_{\text{PIB}}(t+\tau) \rangle_{\text{sp}}$. Consider laser beam projection in an optically homogeneous medium onto a flat, randomly rough target surface, and assume that the characteristic roughness correlation distance, l_S, and the roughness rms amplitude, σ_S, are significantly smaller than the hit-spot size, but larger than the transmitted beam wavelength, λ. In the case of the hit-spot dithering with velocity $\mathbf{v}_S$, one can obtain the following relationship between the correlation function $\Gamma_{\text{PIB}}(\tau)$ and the target-plane intensity distribution $I_T(\mathbf{r})$ [8]:

$$\Gamma_{\text{PIB}}(\tau) = C \int I_T(\mathbf{r}) I_T(\mathbf{r} + \mathbf{v}_S \tau) \mathrm{d}^2\mathbf{r}, \tag{2}$$

where C is a constant. We assumed here that $\sigma_S \geq l_S$ (very rough surface) and that the receiver aperture D_R exceeds the characteristic speckle size, a_{sp}. The dependence described by Eq. (2) can also be utilized for derivation of different SMs. Consider first the PIB signal fluctuation variance that is obtained by substituting $\tau = 0$ into Eq. (2):

$$\sigma_{\text{PIB}}^2 = \Gamma_{\text{PIB}}(0) = \langle \delta J_{\text{PIB}}^2 \rangle = C \int I_T^2(\mathbf{r}) \mathrm{d}^2\mathbf{r}. \tag{3}$$

From Eq. (3) it follows that σ_{PIB}^2 is proportional to the sharpness function $J_2 = \int I_T^2(\mathbf{r}) \mathrm{d}^2\mathbf{r}$, the target-plane metric that is widely used for characterization of image and hit-spot quality [13]. The relationship (3) shows that σ_{PIB}^2 can be considered as an SM for which maximization results in an increase of J_2.

The dependence of the PIB signal fluctuation power spectrum $G_{\text{PIB}}(\omega)$ on the hit-spot size gave rise to a set of SMs that can be easily obtained by band-pass filtering of the received PIB signal [8]:

$$J_{\text{sp}} = \sum_{j=1}^{N} \beta_j P(\omega_j, \Delta_j) = \sum_{j=1}^{N} \beta_j \int_{\omega_j - \Delta_j/2}^{\omega_j + \Delta_j/2} G_{\text{PIB}}(\omega) \mathrm{d}\omega, \tag{4}$$

where $P(\omega_j, \Delta_j)$ with $j = 1, \ldots, N$ indicates a set of N bandpass filters with central frequencies $\{\omega_j\}$ and

bandwidths $\{\Delta_j\}$. Selection of the bandpass filters' parameters and the weighting coefficients $\{\beta_j\}$ in Eq. (4) allows optimization of the SMs' dependence on the target hit-spot intensity distribution. Note that even though the SMs defined in Eqs. (3) and (4) are obtained for speckle-field propagation in vacuum, it was shown that, at least in weak and medium-strength atmospheric turbulence conditions, turbulence has a relatively small impact on the speckle-field statistical characteristics, and the dependence of the SMs on the target hit-spot size is practically unchanged [14]. This property of the speckle field forms the physical basis for the use of the SM AO for beam projection systems operating in atmospheric turbulence conditions.

For experimental validation of the proposed SM sensing and AO techniques, we used a fiber-array-based beam director similar to the one shown in the schematic of Fig. 1(a). The MOPA and fiber-array system operating at wavelength $\lambda = 1064$ nm comprised seven fiber collimators and an SPGD-based phase-locking controller. The system is described in detail in [15,16]. The transmitted collimated beams were focused onto a resolved target (a ceramic plate with flat, rough surface) located at the focal plane of a lens [not shown in Fig. 1(a)] with a focal distance $F = 1.9$ m. The return wave scattered off the target surface was captured by the PIB receiver composed of a lens with a photodetector in its focal plane. The photodetector's output signal, $J_{\mathrm{PIB}}(t)$, was processed by an electronic circuit designed for analog computation of the received signal variance, σ^2_{PIB}, via time averaging of the squared time-varying component of $J_{\mathrm{PIB}}(t)$ over the integration time $\tau_J \approx 1$ μs. The obtained signal (SM, J_{sp}) was sent to the SPGD controller operating at an iteration rate of 73 kHz. In each control channel, the output signal from the SPGD controller was mixed with the 50 MHz modulation signal. The amplitudes of the modulation signals were specially set to provide stair-mode steering of the outgoing combined beam leading to linear displacements of the target hit-spot with an amplitude of about 20 μm.

Different stages of the coherent beam combining experiments are illustrated in Fig. 2, which shows the focal-plane intensity distributions of the combined beam at the target as recorded by a CCD camera that imaged a plane conjugate to the target surface. Figure 2(a) was obtained with both SPGD controller and stair-mode dithering off. Figure 2(b) was recorded during SPGD optimization of the PIB metric J_{PIB}, a setting conventionally used for beam combining on an unresolved target. The beam with uncontrolled phase but stair-mode steering on is depicted in Fig. 2(c). The result of phase locking using SPGD-based maximization of the SM, $J_{\mathrm{sp}} = \sigma^2_{\mathrm{PIB}}$, with stair-mode beam steering is shown in Fig. 2(d). While the PIB metric optimization failed to increase the projected beam power density at the extended target, the use of SM optimization with the SPGD controller resulted in an about twofold increase of the average hit-spot peak irradiance. The results clearly indicate that the described SM AO technique can indeed offer a path towards resolution of a long-standing problem of AO laser beam projection on an extended target with randomly rough surface.

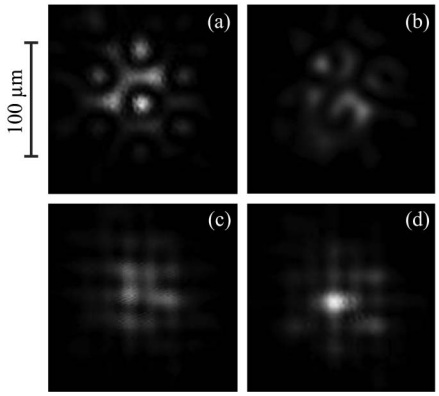

Fig. 2. Intensity patterns at the target surface: (a) no phase control; (b) SPGD phase control using the PIB metric; (c) uncontrolled phase with stair-mode beam dithering on; and (d) SPGD phase control with SM and dithering.

This work was performed in part through collaborative agreement W911NF-09-2-0040 between the United States Army Research Laboratory and the University of Dayton.

References

1. G. Perram, S. Cusumano, R. Hengehold, and S. Fiorino, *An Introduction to Laser Weapon Systems* (DEPS, 2010).
2. P. Merritt, *Beam Control for Laser Systems* (DEPS, 2011).
3. T. R. O'Meara, J. Opt. Soc. Am. **67**, 306 (1977).
4. M. Vorontsov, V. Kolosov, and A. Kohnle, J. Opt. Soc. Am. A **24**, 1975 (2007).
5. J. Pearson, S. Kokorowski, and M. Pedinoff, J. Opt. Soc. Am. **66**, 1261 (1976).
6. M. Vorontsov, V. Karnaukhov, A. Kuz'minskii, and V. Shmal'gauzen, Sov. J. Quantum Electron. **14**, 761 (1984).
7. P. Piatrou and M. Roggemann, Appl. Opt. **46**, 6831 (2007).
8. M. Vorontsov, *Target in the Loop Propagation in Random Media* (FGAN FOM, 2004).
9. M. Vorontsov and G. Carhart, Opt. Lett. **27**, 2155 (2002).
10. J.R. Leger, J. Nilsson, J.P. Huignard, A. Napartovich, T.M. Shay, and A. Shirakawa, eds., IEEE J. Sel. Top. Quantum Electron. **15**, 237 (2009).
11. M. Vorontsov, V. Kolosov, and E. Polnau, Appl. Opt. **48**, A13 (2009).
12. M. Vorontsov, G. Carhart, and J. Ricklin, Opt. Lett. **22**, 907 (1997).
13. R. Muller and A. Buffington, J. Opt. Soc. Am. **64**, 1200 (1974).
14. V. Dudorov, M. Vorontsov, and V. Kolosov, J. Opt. Soc. Am. A **23**, 1924 (2006).
15. T. Weyrauch, M. Vorontsov, G. Carhart, L. Beresnev, A. Rostov, E. Polnau, and J. Liu, Opt. Lett. **36**, 4455 (2011).
16. Optonicus, http://www.optonicus.com.